A Novel Four-Amino Acid Determinant Defines Conformational Freedom within Chorionic Gonadotropin β-Subunits†

Jason A. Wilken‡ and Elliott Bedows*

Department of Biochemistry and Molecular Biology and Eppley Cancer Center, University of Nebraska Medical Center, Omaha, Nebraska 68198

Received November 28, 2006; Revised Manuscript Received January 23, 2007

ABSTRACT: On the basis of apparent molecular mass heterogeneity following reducing versus nonreducing SDS−PAGE, we determined that the β-subunit of macaque (*Macaca fascicularis*) chorionic gonadotropin (mCG-β) is more conformationally constrained than the β-subunit of human chorionic gonadotropin (hCG-β). The amino acid sequences of these two subunits are 81% identical. To determine the conformational variance source, which was not due to glycosylation differences, we generated a series of hCG-β−mCG-β chimeras and identified domains that contributed to CG-β conformational freedom. We discovered that the CG-β 54−101 domain contained a small subdomain, residues 74−77, that regulated the conformational freedom of the β-subunit; i.e., when residues 74−77 were of macaque origin (PGVD), the mutated hCG-β subunit displayed macaque-like conformational rigidity, and when residues 74−77 were of human origin (RGVN), the mutated mCG-β subunit displayed human-like conformational freedom and microheterogeneity. Additionally, CG-β N-terminal domain residues (8, 18, 42, and 46−48) were also found to influence CG-β conformational freedom when residues 74−77 were of human but not macaque origin. The biological significance of the CG-β conformational variance was tested using a biological assay that showed that the hCG-α−hCG-β heterodimer facilitated human CG receptor-mediated cAMP-driven luciferase reporter gene activity in HEK cells nearly 1 order of magnitude more effectively than the hCG-α−mCG-β chimera. Together, these data demonstrate that two essential amino acid residues within a four-amino acid subdomain regulated CG-β conformational freedom and that a conformational difference between hCG-β and mCG-β was recapitulated in the context of receptor-mediated CG heterodimer signal transduction activation.

Chorionic gonadotropin (CG), the placental member of the glycoprotein hormone family, is a noncovalently linked heterodimer consisting of an α-subunit and a β-subunit aligned in a head-to-tail manner. The α-subunit is common to all glycoprotein hormones that function in reproduction (i.e., the gonadotropins), while β-subunits confer biological specificity to each respective family member (*1*). Both human (h) and macaque (*Macaca fascicularis*) (m) CG-β subunits share a similar overall topology of three β-loops stabilized by a ladder of hydrogen bonds and a cystine knot motif. The cystine knot motif is comprised of a unique arrangement of six cysteine residues; with the numbering beginning at the N-terminus of the protein, a disulfide consisting of Cys2 and -5 and one consisting of Cys3 and -6 form a ring structure through which a disulfide consisting of Cys1 and -4 penetrates. CG-β loops 1 and 3 form antiparallel β-strands, while the remaining hairpinlike structure, loop 2, appears as an extended loop connecting β-structural loops 1 and 3 (*2*, *3*).

Our laboratory has previously defined the intracellular kinetic folding pathway of both the hCG[1] α-subunit (*4*) and hCG β-subunits (*5*, *6*) and, more recently, demonstrated that a disulfide exchange occurs as the cystine knot of the CG β-subunit folds (*7*). Identification of disulfide exchange was accomplished by isolating key folding intermediates of mCG-β, a naturally occurring homologue of hCG-β. mCG-β was chosen for these folding studies because both hCG-β and mCG-β are 145 amino acids in length and their amino acid sequences are 81% identical, including all cysteine residues and consensus sequences for both sites of N-linked glycosylation and three of four sites of O-linked glycosylation (see Figure 1) (*8*). During the course of the latter studies (*7*), however, we discovered that hCG-β exhibited more conformational freedom than mCG-β.

In this study, we used a series of molecular and biochemical analyses to compare the nature of the structural elements of h- and mCG-β responsible for the variance in conformational freedom between the respective CG-β subunits. We

† This material is based upon work supported in part by NCI Cancer Center Support Grant P 30 CA36727, NCI Training Grant CA09746 to the Eppley Institute Cancer Center, and a grant from the Nebraska Department of Health (to E.B.). J.A.W. is a recipient of an Emley Fellowship.

* To whom correspondence should be addressed: School of Allied Health Professions, College of Medicine, 984300 Nebraska Medical Center, Omaha, NE 68198-4300. Telephone: (402) 559-6074. Fax: (402) 559-8112. E-mail: ebedows@unmc.edu.

‡ Current address: Department of Obstetrics, Gynecology and Reproductive Sciences, Yale University, 300 George St., Suite 8100, New Haven, CT 06511.

[1] Abbreviations: cAMP, cyclic adenosine monophosphate; hCG, human chorionic gonadotropin; HEK, LH/CG-R human embryonic kidney cells expressing the luteinizing hormone/chorionic gonadotropin receptor; mCG, macaque chorionic gonadotropin; PONDR, predictor of natural disorder; SDS−PAGE, sodium dodecyl sulfate−polyacrylamide gel electrophoresis.

10.1021/bi602449d CCC: $37.00
Published on Web 03/15/2007

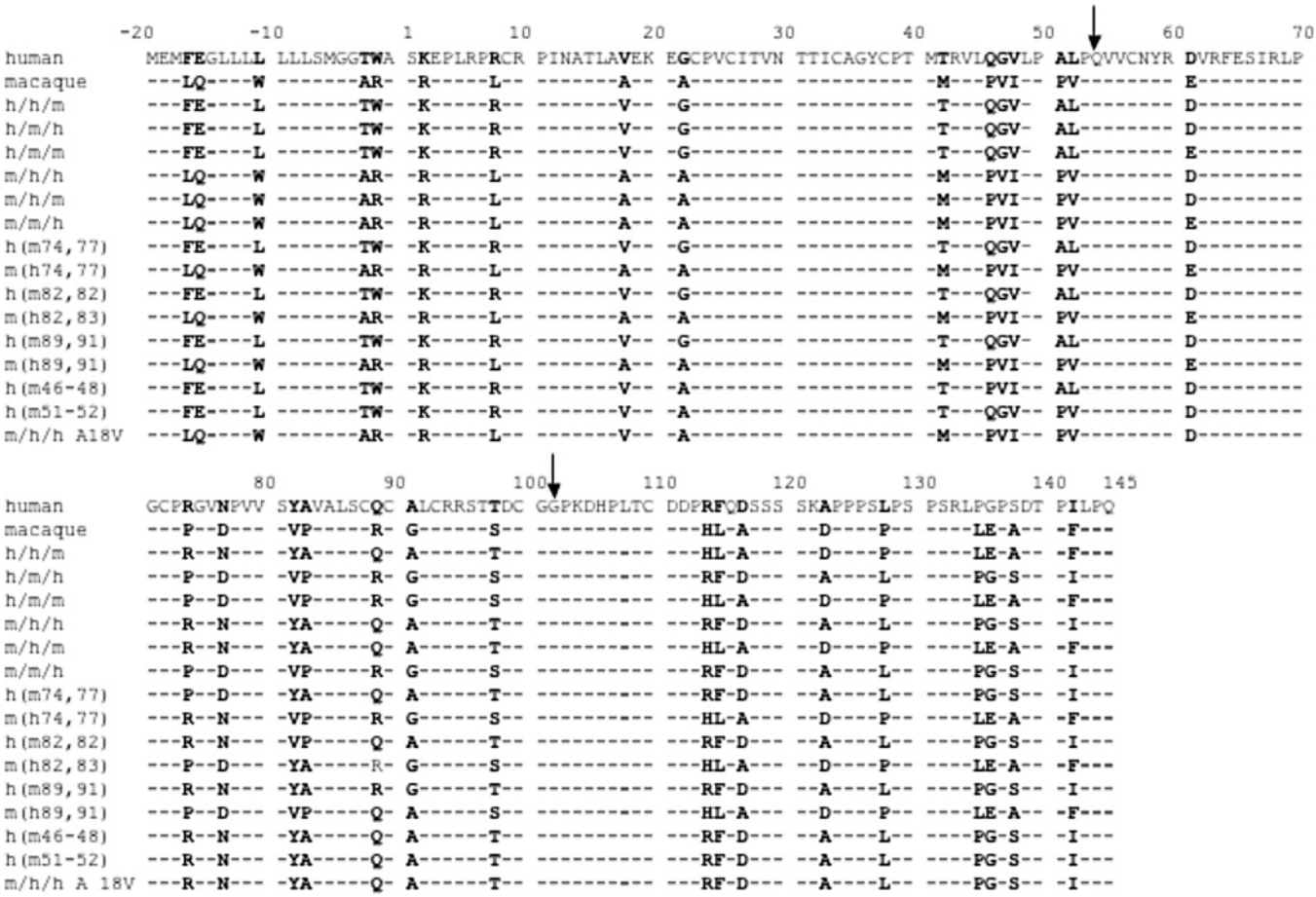

FIGURE 1: Amino acid sequences of CG-β constructs. Shown are the complete primary amino acid sequences of hCG-β (*10*), mCG-β (*8*), and chimeric CG-β constructs. Bold amino acids represent sequences of nonidentity between human and macaque CG-β. The arrows delineate the boundaries between the 1−53, 54−101, and 102−145 domains.

report that two specific amino acid residues were identified in a four-amino acid subdomain that, at least in large part, accounted for these differences.

EXPERIMENTAL PROCEDURES

Construction of hCG-β−mCG-β Chimeras. CG-β chimeras were constructed using "megaprimer" polymerase chain reaction (*9*) with Taq polymerase (Qiagen). The amino acid sequences of hCG-β (*10*), mCG-β (*8*), and all hCG-β−mCG-β chimeras are shown in Figure 1. Primers complementary to two regions of complete identity between hCG-β and mCG-β were used to generate megaprimers that were then used to generate CG-β chimeras, which were cloned into the pGS vector (*11*). Sequences were validated by the Eppley Cancer Center Molecular Biology Core Facility (University of Nebraska Medical Center). Plasmids were prepared using the Maxi Plasmid Kit (Qiagen) according to the manufacturer's protocol.

The amino acid sequence of CG-β was roughly divided into thirds, with the first, second, and third domains comprised of amino acids 1−53, 54−101, and 102−145, respectively. The species identity of each third is represented by an h or m; e.g., chimeras with mCG-β residues 1−53, hCG-β residues 54−101, and mCG-β residues 102−145 are denoted as m-, h-, and mCG-β, respectively. Smaller substitutions generated by site-directed mutagenesis are indicated by species of origin followed by specific amino acid substitutions in parentheses; e.g., hCG-β containing macaque residues 74 and 77 is termed h(m74,77) CG-β. Single-amino acid substitutions are similarly indicated with the identity of the species of origin followed by specific amino acid substitutions in parentheses; e.g., a hCG-β subunit containing macaque residue 18 is termed hCG-β V18A.

Cell Culture. 293T cells were cultured in Dulbecco's modified Eagle's medium (Invitrogen) supplemented with penicillin/streptomycin (100 units/mL and 100 μg/mL, respectively; Invitrogen) and 10% fetal bovine serum (Atlanta Biologicals). CHO cells stably expressing human wild-type hCG-α and mCG-β (*7*) were cultured in Ultraculture (Biowhittaker) supplemented with penicillin/streptomycin and 50 μM methionine sulfoxamine (Sigma). Human embryonic kidney cells stably transfected with the human luteinizing hormone/CG receptor and a cAMP-responsive luciferase reporter (HEK LH/CG-R cells) (*12*) were cultured in low-glucose DMEM (Invitrogen) supplemented with penicillin/streptomycin, 2 mM L-glutamine, and 5% heat-inactivated fetal bovine serum (Invitrogen).

Transient Transfection and Metabolic Labeling of Cells. 293T cells (1.9×10^6) were plated into 60 mm plastic dishes and grown overnight to 70−80% confluency. Plasmid DNA was precipitated as described previously (*13*). The resulting precipitate was added dropwise to the dishes and agitated gently to mix. Cells were incubated for 2 days at 37 °C and used for metabolic labeling. Transfected 293T cells were pulse-labeled for 30 min with L-[^{35}S]cysteine (Perkin-Elmer Life Sciences; ~1100 Ci/mmol; at a concentration of 50−

150 μCi/mL) in serum-free medium lacking cysteine as previously described (*11*), followed by overnight incubation with complete medium lacking radiolabel. Conditioned media were saved for analysis of secreted CG-β subunits.

Immunoprecipitation and Purification of CG-β Subunits. CG-β subunits were precipitated with polyclonal antisera that recognizes all known conformations of hCG-β and mCG-β (*7*, *14*). Immunoprecipitations were carried out at 4 °C overnight with rotation in the dark. Immune complexes were precipitated with protein A-Sepharose (Sigma) and prepared for reversed-phase high-performance liquid chromatography as previously described (*15*). Briefly, protein A-Sepharose beads−antibody−antigen immunocomplexes were washed three times with phosphate-buffered saline containing detergents (1% Triton X-100, 0.5% sodium deoxycholate, and 0.1% SDS) followed by four washes with phosphate-buffered saline lacking detergents. Immunocomplexes were pelleted between washes by centrifugation for 1 min at 2000*g*. To dissociate the Sepharose−antibody−antigen interactions, immunocomplexes were treated with 6 M guanidine HCl (pH 3.0) (sequanal grade; Pierce) for 16−20 h while being rotated at room temperature. Myoglobin (100 μg, Sigma) was added as a carrier. The guanidine eluates were injected onto a Vydac 300 Å C_4 reversed-phase column equilibrated with 0.1% trifluoroacetic acid and eluted using an acetonitrile gradient as described previously (*16*). Fractions were collected in 1 min intervals and quantified by scintillation counting. Fractions containing the major peak were pooled and stored at −20 °C for further characterization.

PAGE Analysis of Conformational Freedom. Radiolabeled CG-β subunits, purified to homogeneity as described above, were resolved by sodium dodecyl sulfate−polyacrylamide gel electrophoresis (SDS−PAGE) as follows. Resolution by nonreducing or reducing SDS−PAGE involved dilution of aliquots into nonreducing sample buffer [125 mM Tris-HCl (pH 6.8) containing 2% SDS, 20% glycerol, and 40 μg/mL bromophenol blue] or reducing buffer (nonreducing gel buffer with 2% β-mercaptoethanol), boiling for 5 min, and loading onto a 5 to 20% gradient polyacrylamide slab gel run by the method described by Laemmli (*17*). Gels were dried in vacuo on filter paper and exposed to a phosphorscreen (Molecular Dynamics) and scanned on a Molecular Dynamics Storm 860 phosphorimager.

CG Bioassay. The ability of CG to induce cyclic adenosine monophosphate (cAMP) production was assayed by a CG-responsive luminescence bioassay (*12*, *18*). Briefly, HEK LH/CG-R cells were seeded into 96-well plates containing growth medium with experimental samples [hCG-α−mCG-β heterodimer, purified as previously described for the mCG-β subunit, at pH 7.4 (*7*) or recombinant hCG standard (Sigma) for 18 h. The concentration of CG heterodimers was determined by densitometry of a Coomassie-stained gel compared to the hCG standard. Cells were lysed with 100 μL of lysis buffer, as described in the manufacturer's instructions (Promega), and incubated with gentle shaking at room temperature for 30 min. Lysate aliquots (25 μL) were mixed with 100 μL of luciferase assay reagent (Promega), and chemiluminescence was measured using a TopCount luminometer (Packard).

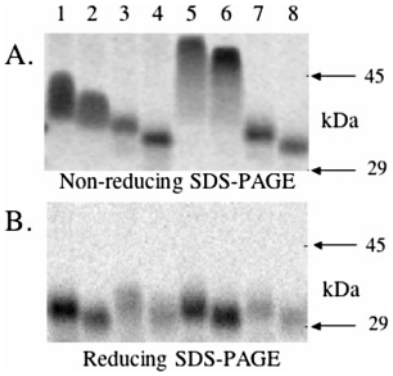

FIGURE 2: Determinant in the 54−101 domain of CG-β modulates CG-β conformational freedom. (A) Purified hCG-β, mCG-β, and selected chimeras assayed by nonreducing SDS−PAGE: lane 1, hCG-β; lane 2, h−h−m CG-β; lane 3, h−m−h CG-β; lane 4, h−m−m CG-β; lane 5, m−h−h CG-β; lane 6, m−h−m CG-β; lane 7, m−m−h CG-β; and lane 8, mCG-β. (B) The same CG-β subunits from panel A were assayed by reducing SDS−PAGE.

RESULTS

h- and mCG-β Display Differential Migration Rates and Microheterogeneity by Nonreducing SDS−PAGE. Methods of resolving proteins on the basis of Stokes radii can distinguish between conformationally free and restrained species (*19*−*23*). Because flexible domains contribute to an abnormally large Stokes radius, a disordered protein can appear to have a larger than expected apparent molecular mass upon gel filtration or gel electrophoresis. Therefore, the respective conformational freedoms of secreted, radiolabeled, and purified h- and mCG-β were resolved by SDS−PAGE under reducing and nonreducing conditions.

A striking difference in the apparent molecular mass of hCG-β (Figure 2A, lane 1) and mCG-β (Figure 2A, lane 8) was observed under nonreducing conditions ($M_r \sim 35000$ and ~ 30000, respectively). Further, hCG-β migrated as a more diffuse, microheterogeneous band than did mCG-β. Under reducing conditions, h- and mCG-β subunits nearly comigrated, with hCG-β (Figure 2B, lane 1) having an ~1 kDa greater apparent molecular mass than mCG-β (Figure 2B, lane 8) because hCG-β contains one additional O-linked glycosylation site (hCG-β Ser138 vs mCG-β Ala138) (*8*). In previous studies that defined the kinetic folding pathway of CG-β, we demonstrated that conformational differences in hCG-β folding intermediates observed under nonreducing SDS−PAGE conditions were not apparent under reducing SDS−PAGE conditions (*11*, *15*, *16*), consistent with results seen in panels A and B of Figure 2.

CG-β Residues 74−77 Represent a Determinant that Modulates the CG-β Conformation. Our results have indicated that mCG-β is more conformationally restrained than hCG. Because the sequences of hCG-β and mCG-β are 81% identical (*8*), we predicted that nonconserved residues in h- and mCG-β influence CG-β conformational freedom. To test this, we constructed a series of chimeras comprised of h- and mCG-β domains to elucidate the sequence−structure relationship(s) of CG-β. CG-β subunits were divided roughly into thirds (residues 1−53, 54−101, and 102−145), and domains were substituted with standard molecular biology techniques to generate the human−macaque CG-β chimeras h−h−m, h−m−h, h−m−m, m−h−h, m−h−m, and m−m−h, shown in Figure 1.

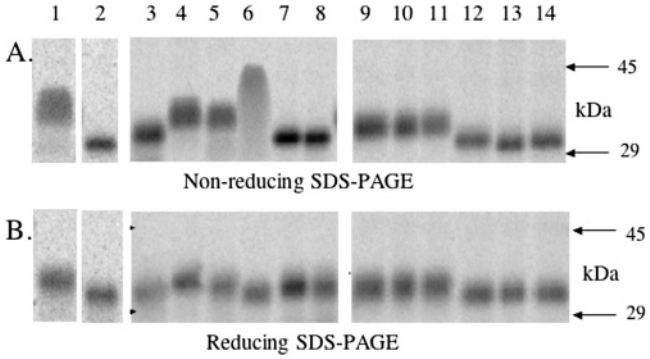

FIGURE 3: CG-β 74−77 domain modulates CG-β conformational freedom. (A) Purified hCG-β 54−101 domain mutants assayed by nonreducing SDS−PAGE: lane 1, hCG-β; lane 2, mCG-β; lane 3, h(m74,77) CG-β; lane 4, h(m82,83) CG-β; lane 5, h(m89,91) CG-β; lane 6, m(h74,77) CG-β; lane 7, m(h82,83) CG-β; lane 8, m(h89,-91) CG-β; lane 9, hCG-β R74P; lane 10, hCG-β R74A; lane 11, hCG-β N77D; lane 12, mCG-β P74R; lane 13, mCG-β P74A; and lane 14, mCG-β D77N. (B) The same CG-β subunits from panel A were assayed by nonreducing SDS−PAGE.

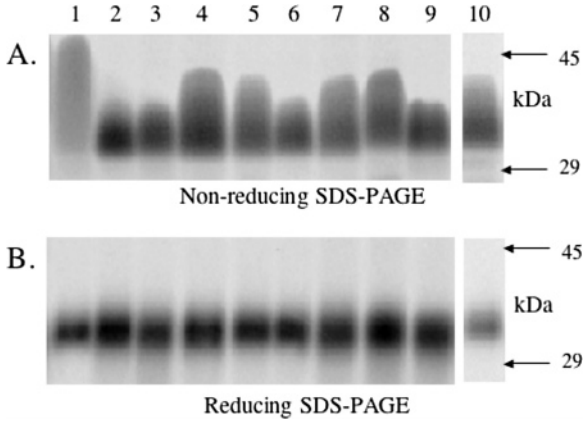

FIGURE 4: Multiple residues of the hCG-β 1−53 domain can influence conformational freedom. (A) Purified hCG-β 1−53 domain mutants assayed by nonreducing SDS−PAGE: lane 1, m−h−h CG-β; lane 2, hCG-β; lane 3, hCG-β K2P; lane 4, hCG-β R2L; lane 5, hCG-β V18A; lane 6, hCG-β G22A; lane 7, hCG-β T42M; lane 8, h(m46−48) CG-β; lane 9, h(m51−52) CG-β; and lane 10, m−h−h CG-β A18V. (B) The same CG-β subunits from panel A were assayed by nonreducing SDS−PAGE.

Plasmids encoding CG-β chimeras were transiently transfected into 293T cells, metabolically labeled as described in Experimental Procedures, and the resulting radiolabeled, purified CG-β subunits were resolved by reducing and nonreducing SDS−PAGE since differences in conformational freedom are revealed under these conditions. As shown in Figure 2A, under nonreducing conditions, we observed that all CG-β subunit chimeras whose middle domain (residues 54−101) contained macaque residues (i.e., h−m−h, h−m−m, m−m−h, and m−m−m CG-β in lanes 3, 4, 7, and 8, respectively) had a reduced apparent molecular mass and microheterogeneity, whereas CG-β subunits whose middle domain contained human residues (i.e., h−h−h, h−h−m, m−h−h, and m−h−m CG-β in lanes 1, 2, 5, and 6, respectively) exhibited increased and highly variable diffusion profiles and apparent molecular masses. That these differences were conformational in nature is demonstrated in Figure 2B, where all subunits migrated similarly on a SDS−PAGE gel under reducing conditions.

Since h- and mCG-β amino acid residues 54−101 differ by only eight amino acids, we further divided this domain into three subdomains. As shown in Figure 1, residues 74, 77, 82, 83, 89, and 91 differ between h- and mCG-β and, therefore, were exchanged, generating constructs h(m74,-77), h(m82,83), h(m89,91), m(h74,77), m(h82,83), and m(89,91) CG-β, where h or m indicates the CG-β species origin and the residues in parentheses represent the substitutions made in these subunits. [Residues 68 and 91 were not tested because the cross-species differences in amino acid identity were conservative (Asp68 vs Glu68 and Thr91 vs Ser91).] h(74,77) CG-β (Figure 3A, lane 3) appeared to be less heterogeneous and to have a lower apparent molecular mass than hCG-β (lane 1), and m(h74,77) CG-β (lane 6) was more heterogeneous and had a higher apparent molecular mass than mCG-β (lane 2). Substituting residues 82 and 83 or 89 and 91 in either CG-β species had no noticeable effect on the migration of these CG-β constructs.

To determine how specific residues within the 74−77 domain affected CG-β conformational freedom, the mutant subunits hCG-β R74P, R74A, and N77D (Figure 3A, lanes 9−11, respectively) as well as mCG-β P74R, P74A, and D77N (Figure 3A, lanes 12−14, respectively) were constructed, purified, and assayed by SDS−PAGE as described above. (Substitution of mCG-β and hCG-β residue 74 with Ala was also tested because of the change in side chain charge and backbone flexibility imparted by R74P and P74R substitutions.) In all cases, the resulting CG-β mutant subunits were similar to mCG-β in terms of microheterogeneity and apparent molecular mass, as determined by nonreducing SDS−PAGE, implying that both hCG-β residues Arg74 and Asn77 are necessary and sufficient to impart hCG-β-like conformational freedom to the CG-β subunit.

Multiple CG-β 1−53 Domain Residues May Also Affect CG-β Conformational Freedom. As shown in Figures 2A and 3A, the m−h−h CG-β, m−h−m CG-β, and m(h74,77) CG-β chimeras appeared to be more heterogeneous than wild-type hCG-β, suggesting that when CG-β residues 74 and 77 were of human origin, additional amino acids within the CG-β 1−53 domain influenced CG-β conformational freedom. To test this, we generated a series of CG-β constructs in which mCG-β residues between positions 1 and 53 were swapped into hCG-β, generating hCG-β K2R, R8L, V18A, G22A, and T42M single-amino acid substitutions (where each substitution represented a change from a wild-type hCG-β residue to the mCG-β residue located at the same position), as well as h(m46−48) CG-β and h(m51−52) CG-β mutants. Purified, radiolabeled CG-β subunits were resolved by reducing and nonreducing SDS−PAGE.

Figure 4A demonstrates that although the mobilities of hCG-β K2R, hCG-β G22A, and h(m51,22) CG-β (lanes 3, 6, and 9, respectively) were indistinguishable from that of wild-type hCG-β (lane 2), hCG-β R8L, V18A, and T42M, and h(m46−48) CG-β (lanes 4, 5, 7, and 8, respectively) migrated with a greater apparent molecular mass and microheterogeneity than wild-type hCG-β (lane 2), and intermediate to that of m−h−h CG-β (lane 1) by nonreducing SDS−PAGE. That all observed differences were conformational in nature is shown in Figure 4B, which reveals that all CG-β subunits migrated similarly under reducing conditions.

Since hCG-β R8L, V18A, T42M, and m46−48 mutants exhibited intermediate apparent molecular mass and micro-

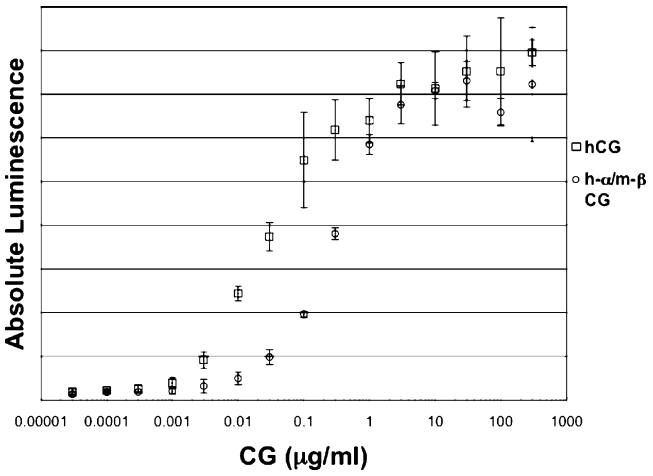

FIGURE 5: Dose−response curve of hCG vs h-α−m-β CG on HEK LH/CG-R cells. HEK LH/CG-R cells were treated with hCG (□) or h-α/m-β CG (○) in half-log concentration increments. Following overnight treatment, cells were lysed and assayed for cAMP-regulated luciferase reporter activity by luminescence assay. All samples were tested in triplicate, with standard deviation bars shown.

heterogeneity compared to those of the m−h−h CG-β chimera, it indicates that the each of these individual substitutions made an independent contribution to the overall conformational freedom of the hCG-β subunit. Further, when we substituted the hV18 residue, which is known to make a major hydrophobic contribution to the earliest folding events of the hCG-β loop 1 domain (*24*), for the mA18 residue in the m−h−h CG-β chimera (thus creating m−h−h CG-β A18V; lane 10), which is less hydrophobic in nature, this construct also displayed an intermediate level of microheterogeneity compared to the m−h−h CG-β chimera and a level of comparable to those of hCG-β R8L, V18A, T42M, and h(m46−48) CG-β subunits. Taken together, our data demonstrate that several individual hCG-β loop 1 and loop 2 amino acids also make a contribution to the conformational freedom of hCG-β but that these contributions are nullified if CG-β residues 74 and 77 are of macaque origin (see Figures 2 and 3).

Conformational Freedom of the CG-β Subunit May Influence the Biological Activity of the CG Heterodimer. Our results have demonstrated that hCG-β and mCG-β differ in their conformational freedom but raise the question of whether these differences in β-subunit conformation are recapitulated in the CG heterodimer. To address this question, we compared the biological activity of the two CG heterodimers each containing the same, human α-subunit. Recombinant hCG (Sigma) and high-performance liquid chromatography-purified CG heterodimer consisting of hCG-α and mCG-β (here termed h-α−m-β CG) were used. Using HEK LH/CG-R cells expressing the human receptor and a cAMP-regulated luciferase reporter gene (*12*), the bioactivities of hCG and h-α−m-β CG were compared as described in Experimental Procedures, generating the dose−response curves shown in Figure 5. Both hCG and h-α−m-β CG exhibited classic receptor−ligand response curves with overlapping minimal and maximal responses and with most of the difference between minimal and maximal responses spanning a two-log difference in CG concentration. hCG and h-α−m-β differed in their EC_{50} values by roughly one-log concentration (∼40 and ∼300 ng/mL, respectively). These data indicate that conformational differences like those seen in the hCG-β and mCG-β subunits were also seen in the respective CG heterodimers.

DISCUSSION

The dimeric glycoprotein hormones hCG and mCG, the sequences of which are >80% identical (*8*), both appear to have parallel physiological functions in pregnancy maintenance (*25*, *26*) and elicit PKA-mediated signal transduction events (*18*). Nonetheless, in the experiments reported here, we demonstrate that the β-subunits of these two CG molecules were conformationally distinct. The differences in conformational freedom between h- and mCG-β suggest that mCG-β, which had a lower apparent molecular mass under nonreducing conditions, was more rod-shaped, while hCG-β was more globular in structure. The nearly identical apparent molecular mass of these two CG-β species seen by reducing SDS−PAGE and our previous demonstration that mCG-β disulfide bond formation parallels that of hCG-β (*7*) suggest that the observed migrational differences between the two subunits under nonreducing conditions were not only conformational in nature but also independent of CG-β domains requiring native disulfide bonds.

Experiments conducted following construction of hCG-β−mCG-β chimeras identified residues of CG-β that were responsible for the conformational variance between the hCG-β and mCG-β subunits. Human residues 54−101 most influenced the overall hCG-β-like conformation; minimization of the 54−101 domain led to the discovery that a four-amino acid stretch, residues 74−77, regulated CG-β conformation, and of this small stretch, only two residues at CG-β codons 74 and 77 differed between h- and mCG-β. Both residues must be of the human type (Arg74 and Asn77) to allow the CG-β subunit to display the flexible hCG-β-like conformation; substitution of macaque-type residues (Pro74 and Asp77) resulted in a subunit with less flexible mCG-β-like characteristics.

The conformational switch attributed to residues 74 and 77 was unexpected. Residues 74−77 of CG-β are found near the apex of loop 3 and in the region of the CG-β 23−72 disulfide bond (see Figure 6A) (*27*, *28*). Substitution of either human residue 74 or 77 with the respective macaque residues results in an overall negative charge for the region (R74P and N77D). We can envision two explanations for how residues 74 and 77 may act to alter the CG-β conformation. According to the hCG crystal structure (*27*, *28*), Lys20 resides within 5 Å of Asn77. Substitution of the human Asn77 with the negatively charged macaque Asp77 appears to be capable of creating a stabilizing salt bridge with Lys20 (see Figure 6). Substitution of the charged human Arg74 with the conformationally constraining macaque Pro74 also appears to decrease the overall flexibility of loop 3, affecting side chain packing between β-loops 1 and 3, thereby affecting the overall conformational stability (see Figure 6). Because conserved residue β73 is also a proline, mCG-β loop 3 contains adjacent proline residues, which would be expected to constrain loop 3 backbone rotational freedom. Thus, it appears that the observed decreased inherent flexibility of mCG-β could arise from either of these amino acid differences, likely being reinforced by the presence of both.

Alignment of the hCG-β crystal structure with the data presented here revealed more unexpected findings. As shown

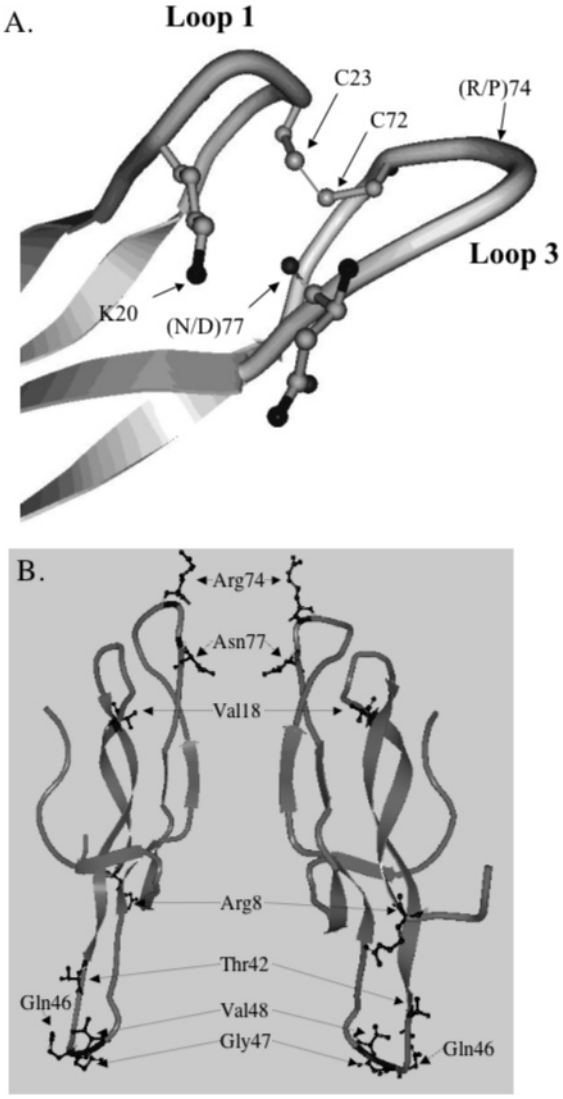

FIGURE 6: Molecular modeling of CG-β. (A) The crystal structure of hCG-β loops 1 and 3, based on the coordinates defined by Wu et al. (*27*), is depicted using MBT Protein Workshop 1.35, with the human and macaque residues 74 and 77 highlighted. Lys20 is also highlighted to demonstrate the potential for electrostatic interaction between Lys20 and Asp77 in mCG-β. Cys23 and Cys72 are highlighted to demonstrate the proximity of the 23−72 disulfide bond. (B) Shown are two views of hCG-β (*27*), rotated 180°, using MBT Protein Workshop 1.35. Residues influencing CG-β conformational freedom when residues β74 and β77 were of human origin (i.e., β-8, -18, -42, -46−48, -74, and -77) are shaded dark.

in Figure 6B, most of the residues that influence hCG-β conformational freedom were found distal to the CG-β core residing, instead, at the periphery of the subunit. Residues 46−48 and 74 are located at the apexes of loops 2 and 3, respectively, while residues 42 and 77, while somewhat closer to the CG-β core, protrude outward into solution. Residue 18 has been previously identified as a component of a CG-β hydrophobic core with Leu16, Ile27, Val29, Ile67, Leu69, Val80, and Tyr82 (*28*), and a substitution from Val18 with Ala could potentially destabilize this core, increasing the conformational freedom of CG-β. This helps explain why m−h−h CG-β exhibited such extensive microheterogeneity compared to either h- or mCG-β, while m−h−h CG-β A18V exhibited less extensive microheterogeneity than m−h−h CG-β (Figure 4A, lanes 1, 2, and 10).

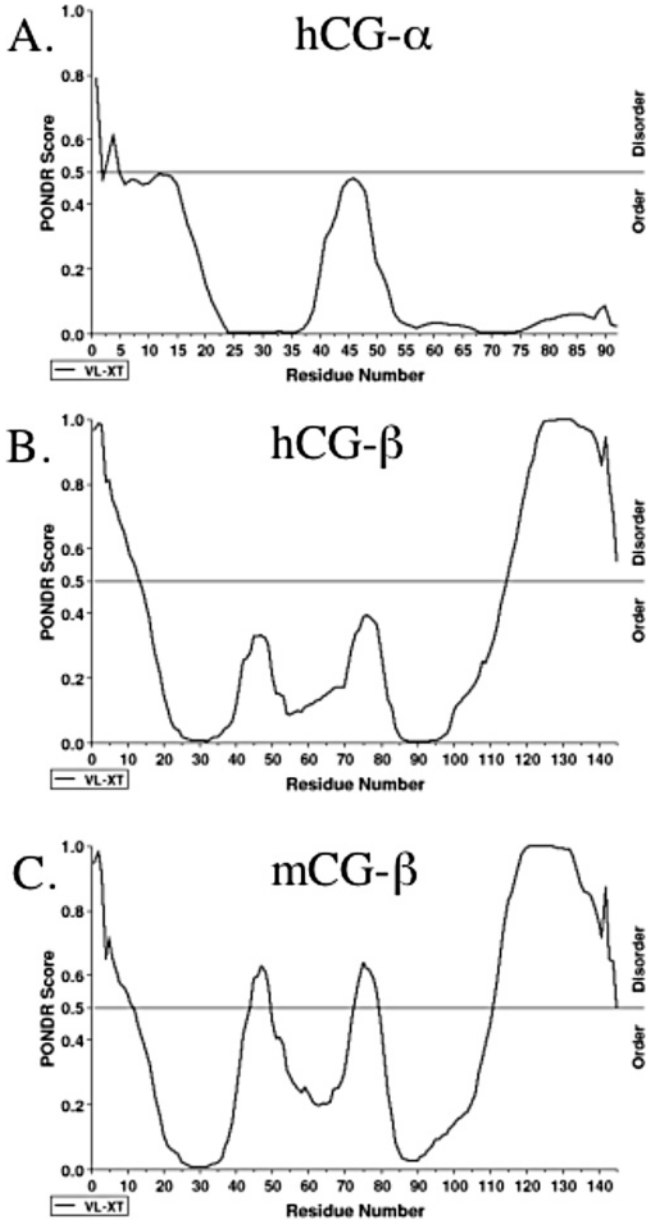

FIGURE 7: PONDR analysis of CG subunit conformational freedom. The computer algorithm PONDR (Molecular Kinetics) (*33*−*35*) VL-XT Predictor was used to predict regions of conformational freedom (or disorder) within CG subunits. (A) PONDR analysis of hCG-α predicted a disordered domain between amino acid residues 35 and 55, in agreement with the findings of Erbel et al. (*29*). (B) PONDR analysis of hCG-β predicted disordered regions spanning residues 40−50, 70−80, and 110−145. No structural data for residues beyond Asp111 are defined by Lapthorn et al. (*28*), in agreement with PONDR analysis. (C) PONDR analysis of mCG-β predicted domains that were similar to those of hCG-β in terms of disorder.

While the crystal structure (*27*, *28*) and the in vivo folding pathway of CG-β (*7*) provide insight into the structural nature of CG, both assume a static final structure and do not take into account the potential flexibility of the molecule. Erbel et al. (*29*) have demonstrated that the solution structure of the heterodimeric partner of CG-β, the α-subunit, possesses extraordinary structural flexibility, or inherent disorder, between residues 33 and 57, with the remainder of the protein exhibiting structurally defined domains. This flexible domain of the α-subunit adopts a more rigid conformation when bound to a glycoprotein hormone β-subunit, and this

conformation varies according to the respective α-subunit binding partner (*27*, *28*, *30*, *31*). This suggests that CG subunits are not static but rather flexible, because of, at least in part, inherent disorder.

We wanted to determine if differences in conformation between hCG-β and mCG-β were recapitulated in the assembled, bioactive CG heterodimer, but we could not address this directly by SDS−PAGE because the noncovalently bound subunits of the CG heterodimer dissociate under SDS−PAGE conditions. Instead, a biological assay was used to investigate the significance of these differences in conformation in the context of an intact heterodimer. As shown in Figure 5, a CG heterodimer containing the mCG-β subunit, while biologically active, was less efficacious than hCG at eliciting a PKA-mediated signal transduction event via the human LH/CG-R. Because hCG and h-α−m-β CG both contain the same α-subunit, the observed difference in biological activity between these heterodimers was attributed to conformational differences in the β-subunits. These results suggest that conformational freedom within the ligand subunits also influenced the signal transduction capabilities of the assembled heterodimer.

Recent advances in the study of protein intrinsic disorder predict that many, if not most, proteins encoded by eukaryotic genomes contain intrinsically disordered regions, if not entire domains (*32*). This estimation was generated by the Predictor of Natural Disorder [PONDR (Molecular Kinetics); www.pondr.com], a commonly cited algorithm for the prediction of regions of intrinsic disorder (*33*−*35*). While PONDR is not capable of predicting interactions spanning long distances in terms of primary amino acid sequence (i.e., interdomain or interprotein disulfide bonds or ionic interactions), it is useful for identifying domains that are potentially disordered. As shown in Figure 7A, PONDR analysis of the amino acid sequence of the α-subunit successfully predicts the existence of an inherently disordered domain that perfectly matches the flexible domain detected by Erbel et al. (*29*). PONDR analysis of hCG-β and mCG-β also provided clues about the conformational freedom of the CG-β subunits. Shown in Figure 7, Panels B and C, the CG-β subunit was predicted to have extensive conformational freedom at its C-terminus, which is in agreement with numerous studies documenting the inherent flexibility of the C-terminal peptide of CG-β (*1*, *28*). PONDR analysis also predicted a disordered domain between residues 1 and 20, and our results demonstrated that residues 8 and 18 regulated CG-β conformational freedom. However, while PONDR predicted that the macaque 70−80 domain would be more disordered than a human 70−80 domain, our results show that the opposite was true. The mechanism by which residues 74 and 77 regulated conformational freedom may involve global interactions in mCG-β not present in hCG-β, which was not be predicted by either PONDR (Figure 7) or SYBYL modeling software (data not shown).

In summary, we have identified the 74−77 subdomain of CG-β loop 3 as a mediator of CG-β conformational freedom, which in mCG-β may result from interactions with residues of β-loop 1 (i.e., a potential salt bridge between residues Lys20 and Asp77 in mCG-β) and/or conformational constraints centered about mCG-β residues Pro73 and Pro74. As mentioned above, the ultimate conformation of all dimeric glycoprotein hormones is reliant on the conformation of their β-subunits, which suggests that CG biological activity could be affected by its inherently disordered domains, which was consistent with the results of our biological activity assay. Perhaps during the course of human evolution, the overall inherent disorder of CG-β increased and, in doing so, provided a selective signaling advantage for hCG following binding of the more flexible ligand to its receptor. This is consistent with the observation that CG-β residues 74−77 are conserved in non-human primates (*8*) and raises further questions about the functional significance of this evolutionary divergence.

ACKNOWLEDGMENT

We thank Dr. John S. Davis for helpful discussions and Claudia MacDonald for her technical assistance.

REFERENCES

1. Pierce, J. G., and Parsons, T. F. (1981) Glycoprotein hormones: Structure and function, *Annu. Rev. Biochem. 50*, 465−495.
2. Sun, P. D., and Davies, D. R. (1995) The cystine-knot growth-factor superfamily, *Annu. Rev. Biophys. Biomol. Struct. 24*, 269−291.
3. Isaacs, N. W. (1995) Cystine knots, *Curr. Opin. Struct. Biol. 5*, 391−395.
4. Darling, R. J., Wilken, J. A., Ruddon, R. W., and Bedows, E. (2001) Intracellular folding pathway of the cystine knot-containing glycoprotein hormone α-subunit, *Biochemistry 40*, 577−585.
5. Ruddon, R. W., Sherman, S. A., and Bedows, E. (1996) Protein folding in the endoplasmic reticulum: Lessons from the human chorionic gonadotropin β subunit, *Protein Sci. 5*, 1443−1452.
6. Ruddon, R. W., and Bedows, E. (1997) Assisted protein folding, *J. Biol. Chem. 272*, 3125−3128.
7. Wilken, J. A., and Bedows, E. (2004) Disulfide bond rearrangement during formation of the chorionic gonadotropin β-subunit cystine knot in vivo, *Biochemistry 43*, 5109−5118.
8. Wilken, J. A., Matsumoto, K., Laughlin, L. S., Lasley, B. L., and Bedows, E. (2002) Comparison of chorionic gonadotropin expression in human and macaque (*Macaca fascicularis*) trophoblasts, *Am. J. Primatol. 56*, 89−97.
9. Sarkar, G., and Sommer, S. S. (1990) The "megaprimer" method of site-directed mutagenesis, *BioTechniques 8*, 404−407.
10. Fiddes, J. C., and Talmadge, K. (1984) Structure, expression, and evolution of the genes for the human glycoprotein hormones, *Recent Prog. Horm. Res. 40*, 43−78.
11. Bedows, E., Huth, J. R., Suganuma, N., Bartels, C. F., Boime, I., and Ruddon, R. W. (1993) Disulfide bond mutations affect the folding of the human chorionic gonadotropin-β subunit in transfected Chinese hamster ovary cells, *J. Biol. Chem. 268*, 11655−11662.
12. Jia, X. C., Perlas, E., Su, J. G., Moran, F., Lasley, B. L., Ny, T., and Hsueh, A. J. (1993) Luminescence luteinizing hormone/choriogonadotropin (LH/CG) bioassay: Measurement of serum bioactive LH/CG during early pregnancy in human and macaque, *Biol. Reprod. 49*, 1310−1316.
13. Darling, R. J., Ruddon, R. W., Perini, F., and Bedows, E. (2000) Cystine knot mutations affect the folding of the glycoprotein hormone α-subunit. Differential secretion and assembly of partially folded intermediates, *J. Biol. Chem. 275*, 15413−15421.
14. Beebe, J. S., Mountjoy, K., Krzesicki, R. F., Perini, F., and Ruddon, R. W. (1990) Role of disulfide bond formation in the folding of human chorionic gonadotropin β subunit into an $\alpha\beta$ dimer assembly-competent form, *J. Biol. Chem. 265*, 312−317.
15. Bedows, E., Huth, J. R., and Ruddon, R. W. (1992) Kinetics of folding and assembly of the human chorionic gonadotropin β subunit in transfected Chinese hamster ovary cells, *J. Biol. Chem. 267*, 8880−8886.
16. Huth, J. R., Mountjoy, K., Perini, F., Bedows, E., and Ruddon, R. W. (1992) Domain-dependent protein folding is indicated by the intracellular kinetics of disulfide bond formation of human chorionic gonadotropin β subunit, *J. Biol. Chem. 267*, 21396−21403.

17. Laemmli, U. K. (1970) Cleavage of structural proteins during the assembly of the head of bacteriophage T4, *Nature 227*, 680−685.
18. Chen, J., Laughlin, L. S., Hendrickx, A. G., Natarajan, K., Overstreet, J. W., and Lasley, B. L. (2003) The effect of 2,3,7,8-tetrachlorodibenzo-p-dioxin (TCDD) on chorionic gonadotrophin activity in pregnant macaques, *Toxicology 186*, 21−31.
19. Kriwacki, R. W., Wu, J., Tennant, L., Wright, P. E., and Siuzdak, G. (1997) Probing protein structure using biochemical and biophysical methods. Proteolysis, matrix-assisted laser desorption/ionization mass spectrometry, high-performance liquid chromatography and size-exclusion chromatography of p21Waf1/Cip1/Sdi1, *J. Chromatogr., A 777*, 23−30.
20. Iakoucheva, L. M., Kimzey, A. L., Masselon, C. D., Smith, R. D., Dunker, A. K., and Ackerman, E. J. (2001) Aberrant mobility phenomena of the DNA repair protein XPA, *Protein Sci. 10*, 1353−1362.
21. Tompa, P. (2002) Intrinsically unstructured proteins, *Trends Biochem. Sci. 27*, 527−533.
22. Uversky, V. N. (1993) Use of fast protein size-exclusion liquid chromatography to study the unfolding of proteins which denature through the molten globule, *Biochemistry 32*, 13288−13298.
23. Dunker, A. K., Lawson, J. D., Brown, C. J., Williams, R. M., Romero, P., Oh, J. S., Oldfield, C. J., Campen, A. M., Ratliff, C. M., Hipps, K. W., Ausio, J., Nissen, M. S., Reeves, R., Kang, C., Kissinger, C. R., Bailey, R. W., Griswold, M. D., Chiu, W., Garner, E. C., and Obradovic, Z. (2001) Intrinsically disordered protein, *J. Mol. Graphics Modell. 19*, 26−59.
24. Silva, R. A. G. D., Sherman, S. A., Perini, F., Bedows, E., and Keiderling, T. A. (2000) Folding Studies on the Human Chorionic Gonadotropin β-Subunit Using Optical Spectroscopy of Peptide Fragments, *J. Am. Chem. Soc. 122*, 8623−8630.
25. Ascoli, M., Fanelli, F., and Segaloff, D. L. (2002) The lutropin/choriogonadotropin receptor, a perspective, *Endocr. Rev. 23*, 141−174.
26. Ho, H. H., Douglas, G. C., Qiu, Q. F., Thirkill, T. L., Overstreet, J. W., and Lasley, B. L. (1997) The relationship between trophoblast differentiation and the production of bioactive hCG, *Early Pregnancy 3*, 291−300.
27. Wu, H., Lustbader, J. W., Liu, Y., Canfield, R. E., and Hendrickson, W. A. (1994) Structure of human chorionic gonadotropin at 2.6 Å resolution from MAD analysis of the selenomethionyl protein, *Structure 2*, 545−558.
28. Lapthorn, A. J., Harris, D. C., Littlejohn, A., Lustbader, J. W., Canfield, R. E., Machin, K. J., Morgan, F. J., and Isaacs, N. W. (1994) Crystal structure of human chorionic gonadotropin, *Nature 369*, 455−461.
29. Erbel, P. J., Karimi-Nejad, Y., De Beer, T., Boelens, R., Kamerling, J. P., and Vliegenthart, J. F. (1999) Solution structure of the α-subunit of human chorionic gonadotropin, *Eur. J. Biochem. 260*, 490−498.
30. Fan, Q. R., and Hendrickson, W. A. (2005) Structure of human follicle-stimulating hormone in complex with its receptor, *Nature 433*, 269−277.
31. Fox, K. M., Dias, J. A., and Van Roey, P. (2001) Three-dimensional structure of human follicle-stimulating hormone, *Mol. Endocrinol. 15*, 378−389.
32. Dunker, A. K., Brown, C. J., Lawson, J. D., Iakoucheva-Sebat, L. M., Vucetic, S., and Obradovic, Z. (2002) The protien trinity: Structure/function relationships that include intrinsic disorder, *ScientificWorldJournal 2*, 49−50.
33. Li, X., Romero, P., Rani, M., Dunker, A. K., and Obradovic, Z. (1999) Predicting Protein Disorder for N-, C-, and Internal Regions, *Genome Inf. Ser. 10*, 30−40.
34. Romero, P., Obradovic, Z., Li, X., Garner, E. C., Brown, C. J., and Dunker, A. K. (2001) Sequence complexity of disordered protein, *Proteins 42*, 38−48.
35. Romero, P., Obradovic, Z., and Dunker, K. (1997) Sequence Data Analysis for Long Disordered Regions Prediction in the Calcineurin Family, *Genome Inf. Ser. 8*, 110−124.

BI602449D